Additive Manufactured W-band Waveguide Components

Mike Coffey[1], Shane Verploegh[1], Stefan Edstaller[2], Shawn Armstrong[3], Erich Grossman[4], Zoya Popović[1]

[1]University of Colorado at Boulder, Boulder, CO 80309, USA
[2]Technische Universitaet Muenchen, Muenchen, Germany
[3]Visser Precision, Denver, CO 80207, USA
[4]NIST, Physical Measurement Lab, Boulder, CO 80305, USA

***Abstract*—This paper presents several W-band (75-110 GHz) WR-10 waveguide components fabricated using both direct metal laser sintering (DMLS) and stereolithography (SLA), in aluminum, nickel and copper alloys and metal-coated plastic (MCP). The RF performance and surface roughness are measured, and the loss due to surface roughness quantified. The measured loss at 95 GHz ranges from 0.055 dB/cm for the copper-plated plastic waveguides to 0.37 dB/cm for the nickel alloy. From a loss budget study, it is found that standard models do not accurately predict loss due to surface roughness for very rough surfaces. This paper presents the current state-of-the-art in available additive manufactured (AM) waveguide components at W-band.**

I. Introduction

The motivation for the recent interest in additive manufacturing (AM) for microwave and millimeter-wave components is the potential for reduced cost and weight, shorter fabrication times and the ability to fabricate assembly geometries not possible with traditional split-block machining techniques [1]. AM is especially attractive for higher frequency metallic waveguide components, and there are a limited number of technologies that can provide conductor printing, most of them with roughness that is considered to be too high for low loss at frequencies above V-band. Published results include low-loss antennas and arrays in the 10-30 GHz range [2], [3], and millimeter-wave components such as W-band filters [4], [5] using a non-commercial tool with post-processing for improved surface finish. The focus of the work presented here is to evaluate various AM fabrication techniques for W-band WR-10 components, especially in terms of loss due to surface roughness. For a uniform analysis, we present results of two simple components, a 10-cm straight waveguide section and a 20-dB directional coupler, using direct metal laser sintering and stereolithography with a variety of materials. Measured S-parameters are used to study the loss due to material conductivity, dimension-introduced mismatch and surface roughness. The roughness is measured and quantified using focus-variation microscopy (FVM).

II. AM for W-band Waveguide Components

The 10-cm straight and 20-dB coupler waveguide components, shown in Fig. 1, are designed in Ansoft HFSS and use standard UG-387 (MIL-DTL-3922/67E) flanges. The DMLS process uses 20-40 μm metal particles that are sintered together with a 400 W Yb laser with a focused finite spot diameter of 200 μm that varies in both size and intensity with output power. Since waveguide features at millimeter-wave frequencies are usually smaller than 200 μm, different laser scanning strategies are employed. Typically, laser output power, spot speed and distance between multiple sintered lines, called hatches, are varied. In this work, two different laser scanning strategies were employed with AlSi10Mg, one with standard settings referred to as A1 and A2 (different manufacturer's standard settings) and one with higher energy density in the perimeter scan, referred to as A3. The trade-off in using higher energy density is reduced feature resolution.

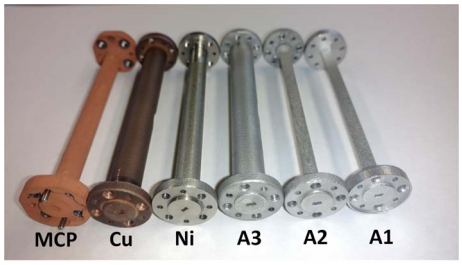

Fig. 1. Straight 10-cm WR-10 waveguides implemented in a variety of materials. From left to right: metal (Cu) coated plastic (MCP), GRCop-84 (Cu), Inconnel 625 (Ni), and 3 AlSi10Mg with different laser settings.

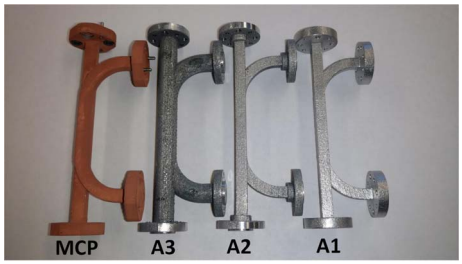

Fig. 2. WR-10 20-dB directional couplers in metal (Cu) coated plastic (MCP) and AlSi10Mg with different laser settings.

As shown in Fig. 3a, the 20-dB coupler design uses 12 identical round coupling holes in a periodic array. The resolution of the DMLS process allows for a minimum wall thickness of 0.3 mm and a minimum feature size of 120 μm. The DMLS fabricated 20-dB coupler design utilized a 0.508 mm hole diameter and a center-to-center hole spacing of 1.375 mm. Because of the SLA process limitations, a second coupler was designed with a larger hole spacing at the expense of bandwidth.

978-1-5090-6360-4/17/$31.00 ©2017 IEEE

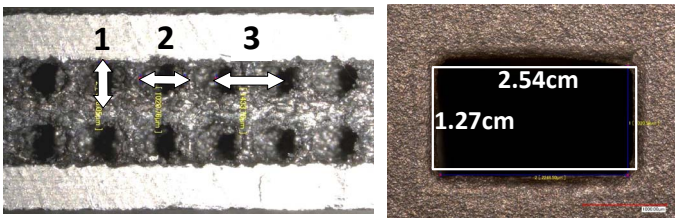

(a) (b)

Fig. 3. a) Micro-photograph of the interior of the 20-dB directional coupler after destructive testing. Various markers show fabricated dimensions: 1) 1020 μm hole diameter 2) a 818 μm hole diameter and 3) a 1433 μm hole-to-hole spacing. b) Aperture dimension deviation for the Cu waveguide. Inset is the correct WR-10 dimensions, as fabricated: 2.25 x1.39 cm.

III. Measured Performance

RF performance and surface roughness characterization is shown in this section for the waveguide components shown in Figs. 1, 2, fabricated in six different materials.

A. RF Performance

The RF performance was measured with an HP8510C and W85104A W-band frequency extenders. The S-parameters of the straight 10-cm WR-10 waveguide sections, in DMLS and SLA and with different materials, are shown in Fig. 4. While $|S_{11}| <$ -10 dB for nearly all components, $|S_{21}|$ varies for each material and the best performance is observed with MCP.

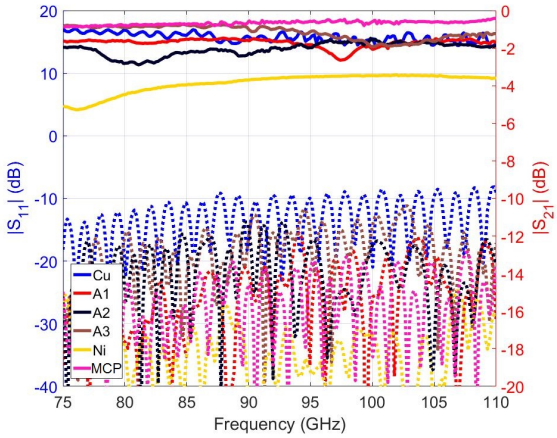

Fig. 4. S-parameter results for the various fabricated WR-10 10-cm waveguide sections. The calibration $dB(|S_{11}|)$ was $<$ -20 dB and it is assumed the standing wave pattern is due to aperture dimension deviation and/or imperfect flange mating.

A summary of $|S_{21}|$ at the center frequency is given below:

	A1	A2	A3	Cu	MCP
$\|S_{21}\|$ (dB)	-1.61	-2.27	-1.02	-1.41	-0.55

The S-parameters of the various WR-10 20-dB couplers are shown in Figs. 5, 6 showing that the best performance is again achieved with MCP. The DMLS AlSi10Mg couplers achieve close to 20 dB coupling ($|S_{31}|$ in Fig. 6) but insertion loss is high ($|S_{21}|$ in Fig. 5.) The A3 AlSi10Mg sample had no through transmission ($dB|S_{21}| \ll 0$) and was excluded from Figs. 5, 6.

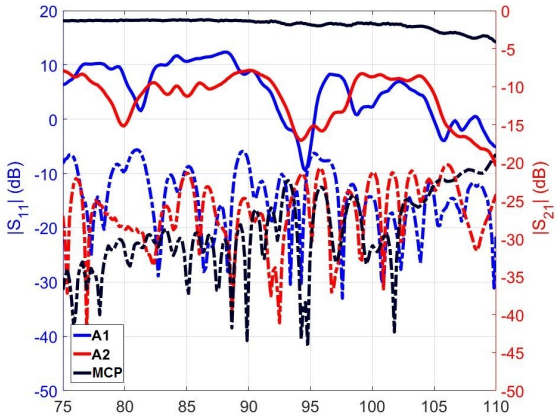

Fig. 5. Measured $|S_{11}|$ and $|S_{21}|$ for the various fabricated WR-10 20-dB directional couplers. $|S_{11}|$ is shown in dashed lines.

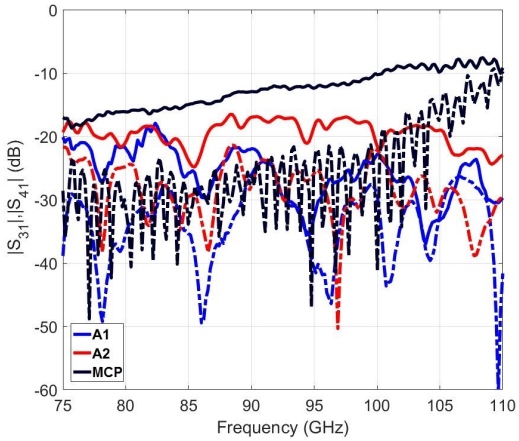

Fig. 6. Measured coupling, $|S_{31}|$, and isolation, $|S_{41}|$, for the various fabricated WR-10 20-dB directional couplers. The isolation, $|S_{41}|$, is shown in dashed lines.

B. Surface Roughness Analysis and Results

Surface roughness and realizable fabrication resolution are the primary limitations in AM millimeter-wave waveguide assemblies [6]. Because minimum feature resolution is often known more accurately than resulting surface roughness, this work focuses on surface roughness characterization. In [7], the spatial bandwidth limitations of FVM, an optical surface finish measurement technique, are analyzed and a measurement protocol is introduced to greatly reduce errors in the technique. The technique described in [7] is used in this work to characterize the surface finish of the AM waveguide components. Shown in Figs. 7a, 7b are the micro-photographs of the waveguide interior surfaces taken during an FVM

978-1-5090-6360-4/17/$31.00 ©2017 IEEE

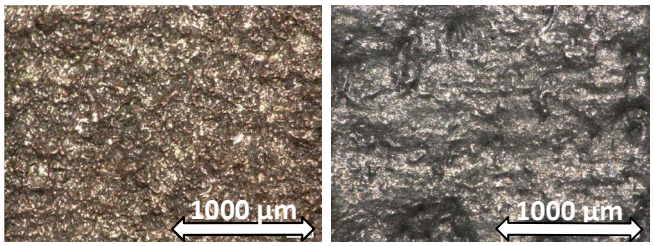

(a) (b)

Fig. 7. a) WR-10 GRCop-84 and b) AlSi10Mg A3 10-cm waveguide section interior surface at 200x zoom.

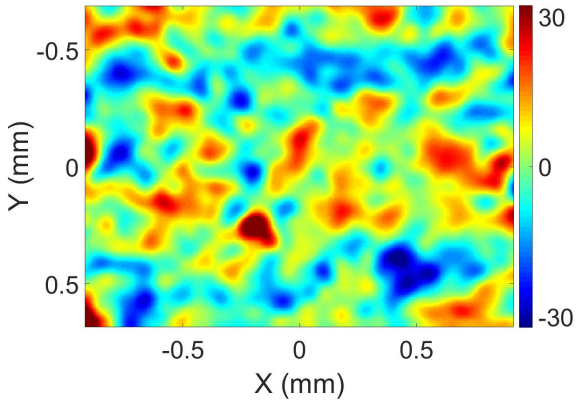

Fig. 8. Measured WR-10 GRCop-84 10-cm waveguide topographical colormap showing $\pm$ 30 μm height deviation.

measurement. Shown in Figs. 8 and 9 is measured deviation in height of the interior of the Cu (GRCop-84) and A3 AlSi10Mg waveguides. The RMS surface roughness σ (often called R_q, R_{RMS} or S_q) and autocorrelation length L (often called Sal) are typically used to characterize the roughness of machined surfaces. The σ value is a measure of the mean deviation of the height and the L value gives an idea of how the deviation is distributed laterally.

In this work, common surface roughness measurement assumptions are made. First, the surface's autocovariance

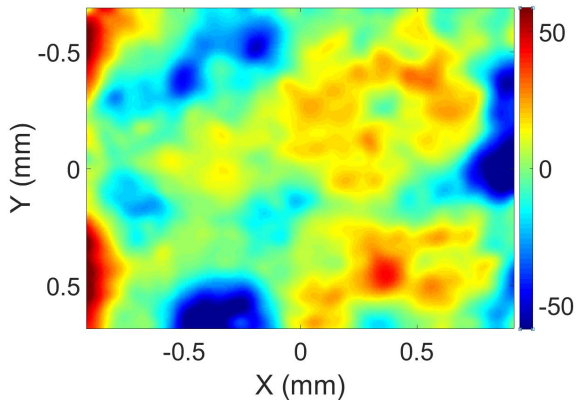

Fig. 9. Measured WR-10 AlSi10Mg A3 10-cm waveguide topographical colormap showing $\pm$ 50 μm height deviation.

function (ACV) is isotropic and exponential and is modeled as:

$$ACV(\tau_x, \tau_y) = \sigma^2 e^{-\tau/L} \quad (1)$$

where σ is the RMS height variation and τ is the lag or displacement and is defined as $\tau = \sqrt{\tau_x^2 + \tau_y^2}$. Second, all height variations, σ, follow a Gaussian distribution. Because the protocol used in the FVM measurements depends on these assumptions to produce accurate results, it is useful to plot the normalized autocorrelation of the measured surface roughness profile, as in Fig. 10.

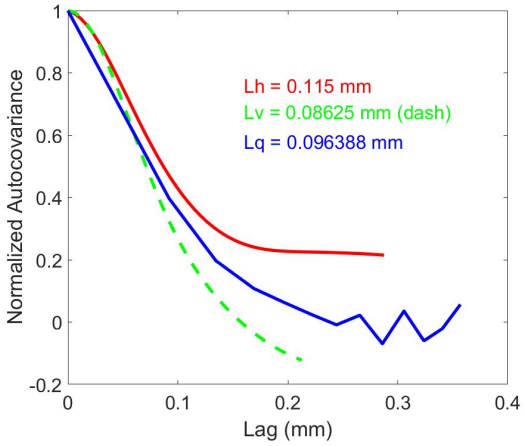

Fig. 10. Normalized autocorrelation Lq, for GRCop-84. Autocorrelation lengths Lh, horizontal, and Lv, vertical show the computed Lq is a good fit to the ACV model before edge effects in the FOV limit affect accuracy.

With the isotropic and exponential behavior of the surface roughness of the fabricated waveguide confirmed, the autocorrelation or autocovariance and RMS surface roughness can accurately be measured. Table I shows the σ and autocorrelation length, L for the various components. Surface roughness testing for the Ni alloy, Inconel 625, was not performed because the material is an extremely durable superalloy and successful destructive testing was not possible.

TABLE I
SUMMARY OF AM WAVEGUIDE SURFACE FINISH CHARACTERISTICS AT 95 GHZ

Material	σ (μm)	L (μm)	α_{meas} (dB/cm)
AlSi10Mg A1	31.70	32.19	0.162
AlSi10Mg A2	12.90	N/A	0.227
AlSi10Mg A3	14.06	144.26	0.103
GRCop-84	12.50	60.85	0.141
Inconel 625	N/A	N/A	0.369
Cu MCP	9.46	199.89	0.055

IV. Analysis and Conclusion

In [8], a commonly used approximation for determining loss due to surface roughness takes the form:

$$C_{SR} = 1 + \frac{2}{\pi} \arctan\left(1.4\left(\frac{\sigma}{\delta}\right)^2\right) \quad (2)$$

978-1-5090-6360-4/17/$31.00 ©2017 IEEE

where δ is the skin depth and C_{SR} is a correction factor applied to the attenuation constant as: $\alpha_{rough} = \alpha_{smooth} C_{SR}$. From the measured surface roughness values in Table I, it is seen that the predicted loss saturates at $2\alpha_{smooth}$ (δ_{Cu} = 0.22 μm at 95 GHz, σ_{Cu} = 58x10^6 S/m). The measured data from the AM waveguide components shows the loss, shown in Table I as α_{meas}, near $4\alpha_{smooth}$, much higher than the predicted $2\alpha_{smooth}$. Because of the widespread use of Eqn. 2 in commercial EM simulators, simulated surface roughness loss is not accurate (predicted losses are too small) for very rough surfaces ($\sigma \gg \delta$). As fabricated, the GRCop-84 waveguide aperture, shown in Fig. 3b, did not meet the specified dimensions of WR-10. The dimension deviation is a source of mismatch loss when connected to the W85104A test set. In Fig. 11, the approximate surface roughness loss for GRCop-84 waveguide is shown. This loss is calculated by subtracting the sum of simulated mismatch loss and simulated loss from the conductivity of copper from the measured $|S_{21}|$.

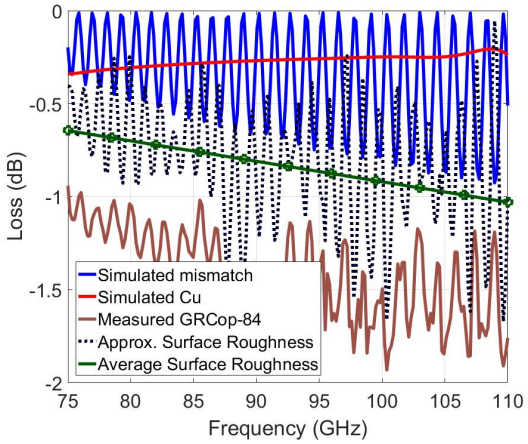

Fig. 11. Different loss mechanisms for GRCop-84 AM waveguide. The surface roughness loss is approximated by subtracting simulated losses (mismatch from aperture dimension deviations and idealized Cu loss) from the measured S-parameter data. Average surface roughness loss (green) is the moving average of the calculated approx. surface roughness loss.

In conclusion, this paper summarizes the current performance of commercially available AM W-band waveguide components. The measured loss of the fabricated components at 95 GHz ranged from 0.055 dB/cm for the MCP waveguides to 0.1 dB/cm for a common AM Al alloy with improved surface finish. The loss mechanisms introduced by the AM process are characterized and it is shown that widely used models for surface roughness loss prediction are not adequate.

ACKNOWLEDGMENT

The authors acknowledge support from DARPA under contract number HR001-16-C-0085. The authors would also like to thank Mr. Bruce Wallace at DARPA for helpful discussions.

REFERENCES

[1] J. Montejo-Garai, Irene O. Saracho-Pantoja, Carlos A. Leal-Sevillano, Jorge A. Ruiz-Cruz, Jesus M. Rebollar, "Design of Microwave Waveguide Devices for Space and Ground Application Implemented by Additive Manufacturing," *2015 Intl. Conf. on Electromagnetics in Adv. Appl.*, 7-11th Sept. 2015

[2] J. Thornton, B. Dalay, D. Smith, "Additive Manufacturing of Waveguides for Ku-band Satellite Communications Antenna" *Electronics Letters*, vol. 48, no. 25, pp. 1607-1608, Dec. 2012

[3] A. Dimitriadis, M. Farve, M. Billod, J. Ansermet, E. de Rijk, "Design and Fabrication of a Lightweight Additive-Manufactured Ka-band Horn Antenna Array," *2016 10th Euro. Conf. on Antennas and Propagation*, 10-15th April, 2016

[4] Mario D' Auria, William J. Otter, Jonathan Hazell, Brendan T. Gillatt, Callum Long-Collins, Nick M. Ridler, Stephan Lucyszyn, "3-D Printed Metal-Pipe Rectangular Waveguides," *IEEE Trans. on Components, Packaging and Manufacturing Tech.*, vol. 5, no. 9, Sept 2015

[5] B. Zhang and H. Zirath, "3D Printed Iris Bandpass Filters for Millimeter-wave Applications, " *Electonics Letters*, vol. 51, no. 22, Oct 2015

[6] B. Zhang, Zhaoyao Zhan, Yu Cao, Heiko Gulan, Peter Linner, Jie Sun, Thomas Zwick, Herbert Zirath, "Metallic 3-D Printed Antennas for Millimeter-and Submillimeter Wave Applications, " *IEEE Trans. on Terahertz Science and Tech.*, vol. 6, no. 4, July 2016

[7] E. N. Grossman, M. Gould, and N.P. Mujica-Schwann, "Robust Evaluation of Statistical Surface Topography Parameters using Focus-Variation Microscopy," *Surface Topography: Metrology and Properties*, vol. 4, no. 3, Sept. 2016

[8] E. Hammerstad and O. Jensen, "Accurate Models of Computer Aided Microstrip Design," *IEEE MTT-S Symposium Digest*, p. 407, May 1980.

978-1-5090-6360-4/17/$31.00 ©2017 IEEE